# SUBBAND MMSE BOUNDS FOR FILTERBANK ADAPTATION IN SYSTEM MODELING NON-UNIFORM SUBBAND ADAPTIVE FILTERS

*Jacob D. Griesbach, Michael Lightner, and Delores M. Etter*

Department of Electrical and Computer Engineering
University of Colorado
Boulder, CO 80309
*griesbac@colorado.edu, lightner@colorado.edu, etter@colorado.edu*

**ABSTRACT**

Minimum mean square error estimators have been developed for non-uniform subband adaptive filters (SAFs) in system modeling configurations. The next step towards practical implementation of non-uniform SAFs involves developing an adaptive algorithm to control the non-uniform filterbank's bandwidths and decimation factors. This paper constructs such an algorithm using subband minimum mean square error (MSE) bounds to suggest decimation factors. A numerical simulation shows that a non-uniform SAF can achieve lower MSE with lower complexity than a equivalent uniform SAF.

## 1. INTRODUCTION

Non-Uniform subband adaptive filters (SAFs) were recently proposed to outperform equivalent uniform SAFs due to their increased flexibility [1]. Since uniform SAFs are widely used for a variety of applications, most notably echo cancellation, an increase in SAF performance could be very beneficial. However, an adaptive algorithm to control the non-uniform filterbank has yet to be rigorously developed. With an adaptive algorithm to control the non-uniform filterbank, the non-uniform SAF can be compared against an equivalent uniform SAF. To compare the performance of SAFs, three issues must be analyzed: mean square error (MSE) after convergence, convergence time / tracking ability, and computational complexity.

A non-uniform SAF in a system modeling configuration is shown in Figure 1. It should be noted that the decimation blocks shown in the figure imply a *multiplication by the decimation factor,* $D_m$. This is needed to ensure proper reconstruction while allowing the passband magnitudes for the analysis and synthesis filters to be equal to 1. (A comment on notation: this paper will utilize the scalar $j$ as an index variable, while $\jmath$ will be used to represent the imaginary unit, $\jmath = \sqrt{-1}$. An overbar signifies conjugation.)

In the following section, upper bounds for the subband minimum mean square error (MMSE) will be derived. Section 3 will utilize these bounds to construct an adaptive algorithm which controls the filterbank of a non-uniform SAF. Section 4 will follow with simulations to compare non-uniform and uniform SAFs..

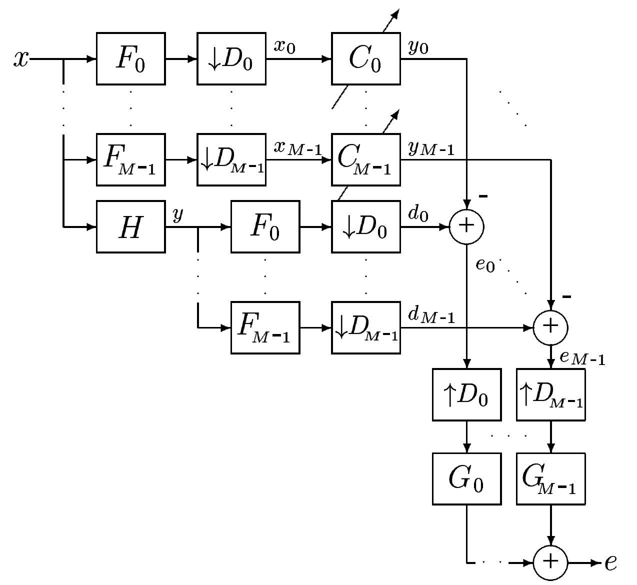


**Fig. 1**. A System Modeling Non-Uniform Subband Adaptive Filter

## 2. SUBBAND MMSE UPPER BOUNDS

Rigorous MMSE estimators have been derived for non-uniform SAF subband and fullband MSEs in both the time and spectral domains [2, 3]. Assuming the input signal spectrum is white ($S_{x,x}(\theta) = 1$), the spectral domain subband MMSE estimator for a subband with a non-causal adaptive filter is given by

$$S_{e_m,e_m} = \sum_{i=1}^{D_m-1} \sum_{j=1}^{D_m-1} H_{m,i}\left[S_{m,m,i,j} - S_{m,m,i,0} S^{-1}_{m,m,0,0} S_{m,m,0,j}\right] \bar{H}_{m,j} \tag{1}$$

where $S_{m,m,i,j}(\theta)$ is the $m^{\text{th}}$ subband's $i^{\text{th}}$ and $j^{\text{th}}$ polyphase input signal cross-spectrum, and $H_{m,i}(e^{\jmath\theta})$ denotes the DTFT of the $i^{\text{th}}$ polyphase component of the unknown system when decimated by $D_m$. $S_{m,m,i,j}(\theta)$ can be shown to be given by

$$\begin{aligned} S_{m,m,i,j}(\theta) &= S_{x_{m,i},x_{m,j}}(\theta) \\ &= D_m \sum_{k=0}^{D_m-1} S_{u_m,u_m}(\tfrac{\theta-2\pi k}{D_m}) \mathrm{e}^{-\jmath\frac{(\theta-2\pi k)(i-j)}{D_m}}, \end{aligned} \quad (2)$$

where $S_{u_m,u_m}(\theta) = |F_m(\mathrm{e}^{\jmath\theta})|^2$ and $0 \le i, j \le D_m$-1.

The non-causal adaptive filter bound is utilized for its simplicity. Although, non-causal adaptive filters are not practical in real-time, (1) forms a lower bound for FIR adaptive filters, since FIR filters can be considered a special case of non-causal filter. With FIR adaptive filters, the subband adaptive filter can be shown to model the first $N$ time-domain coefficients of the unknown system, $h(n) = \int_{-\pi}^{\pi} H(\mathrm{e}^{\jmath\theta})\mathrm{e}^{\jmath n\theta} d\theta$, $0 \le n \le N$-1 where $N$ denotes the fullband length of the subband adaptive filter. (1) will be a tight lower bound if $N$ is greater than the filter length of the analysis filters (which is normally the case).

*For the remainder of this section, all of the equations will pertain to the $m^{th}$ subband. Therefore, to avoid cumbersome notation, the $m$ subscript will be dropped.*

Redistributing the summations of (1) and multiplying by $S_{0,0}(\theta)$ gives

$$\begin{aligned} S_{e,e}S_{0,0} &= \sum_{i=1}^{D\text{-}1} |H_i|^2 \left(S_{0,0}^2 - |S_{i,0}|^2\right) \\ &+ \sum_{i=1}^{D\text{-}1} \sum_{j=i+1}^{D\text{-}1} 2\mathcal{R}\varepsilon \left\{ H_i \left(S_{i,j} - S_{i,0}S_{0,0}^{-1}S_{0,j}\right) \bar{H}_j \right\} \end{aligned} \quad (3)$$

where $\mathcal{R}\varepsilon$ denotes the real part operation. Using (2),

$$\begin{aligned} &\tfrac{S_{0,0}^2 - |S_{i,0}|^2}{D^2} = \\ &= \sum_{k=0}^{D\text{-}1}\sum_{l=0}^{D\text{-}1} S_{u,u}(\tfrac{\theta-2\pi k}{D}) S_{u,u}(\tfrac{\theta-2\pi l}{D}) \left(1 - \mathrm{e}^{\frac{-\jmath(l-k)2\pi i}{D}}\right) \\ &= 2\sum_{k=0}^{D\text{-}1}\sum_{l=k+1}^{D\text{-}1} S_{u,u}(\tfrac{\theta-2\pi k}{D}) S_{u,u}(\tfrac{\theta-2\pi l}{D}) (1\text{-}\cos(\tfrac{(k-l)2\pi i}{D})) \\ &= 4\sum_{k=0}^{D\text{-}1}\sum_{l=k+1}^{D\text{-}1} S_{u,u}(\tfrac{\theta-2\pi k}{D}) S_{u,u}(\tfrac{\theta-2\pi l}{D}) \sin^2(\tfrac{(k-l)\pi i}{D}). \end{aligned} \quad (4)$$

Using similar summation redistributions and trigonometric identities,

$$\begin{aligned} &\tfrac{S_{i,j}S_{0,0} - S_{i,0}S_{0,j}}{D^2} = \\ &= \sum_{k=0}^{D\text{-}1}\sum_{l=k+1}^{D\text{-}1} 4S_{u,u}(\tfrac{\theta-2\pi k}{D}) S_{u,u}(\tfrac{\theta-2\pi l}{D}) \mathrm{e}^{-\frac{\jmath(i-j)\theta}{D}} \\ &\cdot\ \mathrm{e}^{-\frac{\jmath(k+l)(j-i)\pi}{D}} \sin(\tfrac{(k-l)i\pi}{D}) \sin(\tfrac{(k-l)j\pi}{D}). \end{aligned} \quad (5)$$

Substituting (4) and (5) back into (3), factoring, and dividing again by $S_{0,0}$ gives

$$S_{e,e}(\theta) = 4D^2 \sum_{k=0}^{D\text{-}1}\sum_{l=k+1}^{D\text{-}1} \frac{S_{u,u}(\frac{\theta-2\pi k}{D}) S_{u,u}(\frac{\theta-2\pi l}{D})}{S_{0,0}(\theta)} \rho(\theta, k, l) \quad (6)$$

where

$$\rho(\theta, k, l) = \left| \sum_{i=1}^{D-1} H_i(\theta) \sin\left(\frac{(k-l)\pi i}{D}\right) \mathrm{e}^{-\frac{\jmath i\theta}{D}} \mathrm{e}^{\frac{\jmath(k+l)i\pi}{D}} \right|^2. \quad (7)$$

Here, it is interesting to note that (6), without $\rho$ (i.e. $\rho(\theta, k, l) = 1$), can be bounded. The spectra of $S_{u,u}(\theta)$ and $S_{0,0}(\theta)$ are known since they are merely a function of the subband analysis filter, $F(\theta)$. Therefore, it can be shown that if a constituent filterbank is used to generate the non-uniform analysis and synthesis filters, as outlined in [1],

$$\sum_{k=0}^{D\text{-}1}\sum_{l=k+1}^{D\text{-}1} \frac{S_{u,u}(\frac{\theta-2\pi k}{D}) S_{u,u}(\frac{\theta-2\pi l}{D})}{S_{0,0}(\theta)} \le L_m^2 A_s^2 \quad (8)$$

where $L_m$ is the number of constituent filters in the $m^{\text{th}}$ subband and $A_s$ is the maximum stopband amplitude of the pseudo-QMF prototype filter.

Next, (6) will be simplified by bounding it from above. Using various bounding techniques will yield three bounds which each require different amounts of knowledge regarding the unknown system.

### 2.1. $\infty$ Norm Bound

The spectrum of the $i^{\text{th}}$ polyphase component of the unknown system, $H_i(\theta)$, is given by

$$H_i(\theta) = \frac{1}{D} \sum_{j=0}^{D-1} H\left(\frac{\theta - 2\pi j}{D}\right) \mathrm{e}^{-\frac{\jmath(\theta-2\pi j)i}{D}}. \quad (9)$$

where $H(\theta)$ is the spectrum of the unknown system. Applying the triangle inequality and (9) to (7) yields

$$\begin{aligned} &\rho(\theta, k, l) = \\ &\le \left( \sum_{i=1}^{D-1} \left| H_i(\theta) \sin(\tfrac{(k-l)\pi i}{D}) \mathrm{e}^{-\frac{\jmath\theta i}{D}} \mathrm{e}^{\frac{\jmath(k+l)i\pi}{D}} \right| \right)^2 \\ &= \left( \tfrac{1}{D} \sum_{i=1}^{D-1}\sum_{j=0}^{D-1} \left| H(\tfrac{\theta-2\pi j}{D}) \sin(\tfrac{(k-l)\pi i}{D}) \right| \right)^2 \\ &\le \left( \tfrac{1}{D} \sum_{i=1}^{D-1}\sum_{j=0}^{D-1} \| \, |H(\theta)| \, \|_\infty \right)^2 \\ &= (D-1)^2 \, \| \, |H(\theta)| \, \|_\infty^2 . \end{aligned} \quad (10)$$

This implies that

$$\text{MMSE} \le \left( 2D(D-1)L_m A_s \, \| \, |H(\theta)| \, \|_\infty \right)^2 \quad (11)$$

where the subband MMSE $= \frac{1}{2\pi}\int_{-\pi}^{\pi} S_{e,e}(\theta) d\theta$.

This bound illustrates that, in general, lower decimation factors and fewer constituents decrease the subband MMSE.

### 2.2. Min-Max Bound

Simply applying the triangle inequality to (7) without (9) gives

$$\rho(\theta,k,l) \leq \left(\sum_{i=1}^{D\text{-}1} |H_i(\theta)|\right)^2. \tag{12}$$

Then,

$$\text{MMSE} \leq \frac{1}{2\pi}\int_{-\pi}^{\pi} 4D^2 \left(\sum_{i=1}^{D\text{-}1} |H_i(\theta)|\right)^2 L_m^2 A_s^2 d\theta$$

$$= 4D^2 L_m^2 A_s^2 \frac{1}{2\pi}\int_{-\pi}^{\pi} \sum_{i=1}^{D\text{-}1}\sum_{j=1}^{D\text{-}1} |H_i(\theta)||H_j(\theta)| d\theta. \tag{13}$$

Let

$$\begin{aligned}\eta &= \arg\max_i \left\{\frac{1}{2\pi}\int_{-\pi}^{\pi} |H_i(\theta)|^2 d\theta\right\} \\ &= \arg\max_i \left\{\sum_{n=0}^{\infty} h_i^2(n)\right\}\end{aligned} \tag{14}$$

where $H_i(\theta) = \frac{1}{2\pi}\int_{-\pi}^{\pi} h_i(n) \mathrm{e}^{-\jmath\theta n} dn$. This implies that

$$\begin{aligned}\text{MMSE} &\leq 4D^2 L_m^2 A_s^2 \frac{1}{2\pi}\int_{-\pi}^{\pi} \sum_{i=1}^{D\text{-}1}\sum_{j=1}^{D\text{-}1} |H_\eta(\theta)|^2 d\theta \\ &= 4D^2 L_m^2 A_s^2 \sum_{i=1}^{D\text{-}1}\sum_{j=1}^{D\text{-}1} ||h_\eta||_2^2 \\ &= 4D^2 (D\text{-}1)^2 L_m^2 A_s^2 ||h_\eta||_2^2.\end{aligned} \tag{15}$$

This bound is clearly tighter than the $\infty$ norm bound, but requires more knowledge of the unknown system. This bound shows that, in general, the subband MSE can be minimized by choosing the decimation factor which minimizes the maximum unknown polyphase component power.

### 2.3. Cauchy-Schwartz Bound

Applying the Cauchy-Schwartz inequality to (13) gives

$$\text{MMSE} \leq 4D^2 L_m^2 A_s^2 \sum_{i=1}^{D\text{-}1}\sum_{j=1}^{D\text{-}1} \frac{1}{2\pi} ||\,|H_i(\theta)|\,||_2 ||\,|H_j(\theta)\,||_2. \tag{16}$$

However,

$$|| \, |H_i(\theta)| \, ||_2 = \left(\int_{-\pi}^{\pi} |H_i(\theta)|^2 d\theta\right)^{\frac{1}{2}}$$

$$= \left(\sum_{n=0}^{\infty} h_i^2(n)\right)^{\frac{1}{2}} \sqrt{2\pi} = ||h_i||_2 \sqrt{2\pi} \tag{17}$$

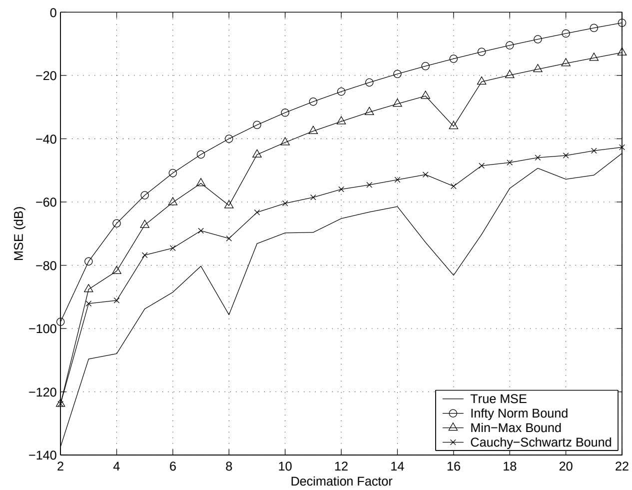


**Fig. 2**. Subband Bounds with $L_m = 2$ and Bandstop Unknown System

which shows that

$$\text{MMSE} \leq 4D^2 L_m^2 A_s^2 \sum_{i=1}^{D\text{-}1}\sum_{j=1}^{D\text{-}1} ||h_i||_2 ||h_j||_2. \tag{18}$$

This bound is tighter than the min-max bound, but requires complete knowledge of the unknown system. It suggests that the subband MSE can best be minimized by choosing a decimation factor that minimizes the joint power of all the unknown polyphase components.

Figure 2 illustrates the bounds for the bandstop unknown system shown in Figure 4 and compares them to the actual theoretical FIR MMSE as derived in [3, 4]. It is interesting to note that the min-max bound identifies the MSE peaks best, while the Cauchy-Schwartz bound is tightest overall.

## 3. ADAPTIVE FILTERBANK ALGORITHM

Before an adaptive algorithm can be developed to control the non-uniform filterbank, practical filterbank constraints must be considered. Assuming the SAF utilizes a separate DSP per subband, it is reasonable to assume that any given subband cannot exceed the complexity it would have if it were part of an equivalent uniform SAF. Since complexity is a function solely based on the chosen decimation factor, the minimum decimation factor must then be greater than or equal to the decimation factor associated with an equivalent uniform SAF. Furthermore, if the error is to be evenly distributed across all the subbands, significant subbands should be allocated uniformly to maximize the number of possible decimation factor choices for all subbands and minimize complexity.

With the above constraints and reasoning, an adaptive algorithm can be identified. Since no apriori knowledge is

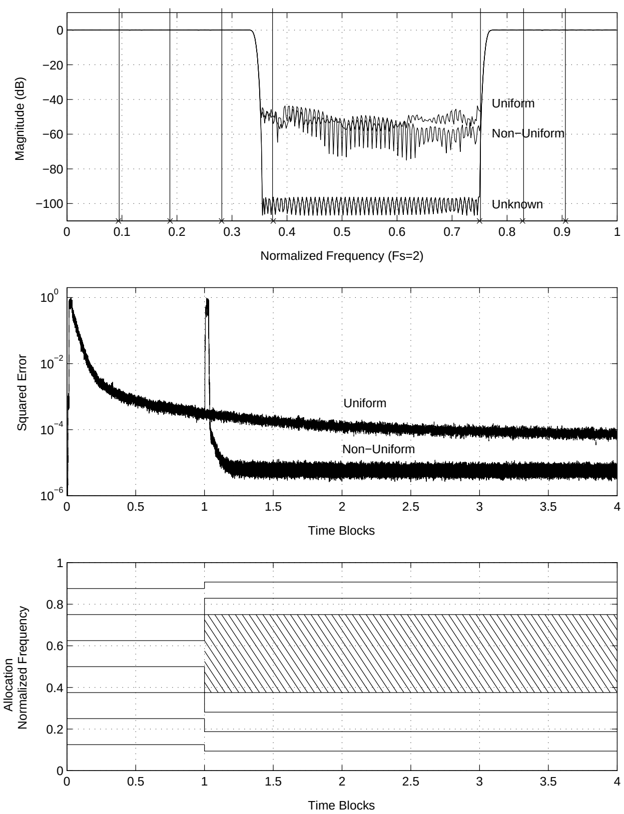


**Fig. 3**. Numerical Simulation Results

| | MSE | Complexity |
|---|---|---|
| Non-Uniform | $5.50 \times 10^{-6}$ | 823.2 |
| Uniform | $8.14 \times 10^{-5}$ | 921.3 |

**Table 1**. MSE and Complexity Comparison

assumed, begin with a uniform SAF. When the subbands have sufficiently converged, subbands can be probed to identify which subbands contain power. Subbands with power below the noise floor can be eliminated and joined with neighboring subbands with similar power. Then the remaining significant bandwidth can be uniformly redistributed over the significant subbands. This tends to reduce the bandwidth of significant subbands allowing them to be decimated with higher decimation factors. Finally, using the fullband estimate of the unknown system, the Cauchy-Schwartz (or alternatively the min-max) bound can be used to identify the best decimation factor from the possible decimation factor choices for each subband.

## 4. NUMERICAL SIMULATION

Non-uniform and uniform SAFs are simulated, each with $M = 8$ subbands. The subband analysis and synthesis filters are composed from a constituent filterbank with 64 uniform filters [1]. A 513 tap bandstop filter was used as the unknown system. $D = 13$ for the uniform SAF and represents the minimum decimation factor allowed for the non-uniform SAF. The adaptive filters in each subband were evaluated using NLMS ($\tilde{\mu} = 1$).

Figure 3 illustrates the results of the simulations. The top graph in Figure 3 shows the final converged spectra of the non-uniform and uniform SAFs against the spectrum of the unknown system. Grey vertical lines illustrate the bandwidths of the non-uniform filterbank after adaptation. The middle graph shows the output squared error over time for both graphs. A time block is equal to $2^{14}$ input samples. An non-uniform SAF error spike results when the filterbank adapts with duration equal to the time necessary to refill the analysis and adaptive taps with valid data. The MSE for the non-uniform SAF clearly outperforms the uniform SAF after the filterbank adapts. The final graph in Figure 3 illustrates the bandwidth allocation of the non-uniform filterbank over time. The shaded areas are stopband subbands.

Table 1 numerically shows the MSE for both the non-uniform and uniform SAFs. The complexity (measured in real multiplies per fullband input sample) of both filters is also listed.

The results show that a non-uniform SAF can be implemented which achieves lower MSE with lower complexity than an equivalent uniform SAF.

## 5. CONCLUSIONS / FUTURE WORK

This research developed bounds for the subband MSE which could be easily evaluated for non-uniform filterbank parameters. These bounds allow one to construct an algorithm to control the non-uniform filterbank associated with a non-uniform SAF. A numerical simulation shows that the non-uniform SAF obtains a better MSE with lower complexity than an equivalent uniform SAF. Future analysis will compare the convergence rates for a complete performance comparison.

## 6. REFERENCES

[1] Jacob D. Griesbach, Tamal Bose, and Delores M. Etter, "Non-uniform filterbank bandwidth allocation for system modeling subband adaptive filters," in *ICASSP–99*, 1999, vol. 3, pp. 1473–1476.

[2] Jacob D. Griesbach, Michael Lightner, and Delores M. Etter, "Spectral domain mmse estimators for non-uniform system modeling subband adaptive filters," in $34^{th}$ *Asilomar Conference on Signals, Systems, and Computers*, Pacific Grove, CA, October 29–1 2000, IEEE.

[3] Jacob D. Griesbach, Michael Lightner, and Delores M. Etter, "Mean square analysis of non-uniform subband adaptive filters for system modeling," *IEEE Transactions on Signal Processing*, Submitted August 2000.

[4] Yoshihiro Ono, Kiyoshi Nishikawa, and Hitoshi Kiya, "An equivalent model for subband adaptive system and analysis of its performance," *Electronics and Communications in Japan, Part 3*, vol. 78, no. 9, pp. 55–66, 1995.